

Rapid green synthesis of silver nanoparticles from *Chrysanthemum indicum* L and its antibacterial and cytotoxic effects: an in vitro study

Selvaraj Arokiyaraj¹
 Mariadhas Valan Arasu²
 Savariar Vincent³
 Nyayirukannaian Udaya
 Prakash⁴
 Seong Ho Choi⁵
 Young-Kyoon Oh¹
 Ki Choon Choi²
 Kyoung Hoon Kim^{1,6}

¹Department of Animal Nutrition and Physiology, National Institute of Animal Science, Rural Development Administration, Suwon, Republic of Korea; ²Grassland and Forage Division, National Institute of Animal Science, Rural Development Administration, Seonghwan-Eup, Cheonan-Si, Chungnam, Republic of Korea; ³Center for Environmental Research and Development, Loyola College, Chennai, India; ⁴Research and Development, Vel Tech Dr RR and Dr SR Technical University, Chennai, India; ⁵Department of Animal Science, Chungbuk National University, Chungbuk, Republic of Korea; ⁶Department of Animal Science, Seoul National University, Pyeongchang, Republic of Korea

Correspondence: Kyoung Hoon Kim
 Department of Animal Nutrition and Physiology, National Institute of Animal Science, Rural Development Administration, 126 Suin-ro Gwonseon-gu Suwon-si Gyeonggi-do 441-707, Republic of Korea
 Tel +82 102 315 0434
 Email kh665@korea.kr

Abstract: The present work reports a simple, cost-effective, and ecofriendly method for the synthesis of silver nanoparticles (AgNPs) using *Chrysanthemum indicum* and its antibacterial and cytotoxic effects. The formation of AgNPs was confirmed by color change, and it was further characterized by ultraviolet-visible spectroscopy (435 nm). The phytochemical screening of *C. indicum* revealed the presence of flavonoids, terpenoids, and glycosides, suggesting that these compounds act as reducing and stabilizing agents. The crystalline nature of the synthesized particles was confirmed by X-ray diffraction, as they exhibited face-centered cubic symmetry. The size and morphology of the particles were characterized by transmission electron microscopy, which showed spherical shapes and sizes that ranged between 37.71–71.99 nm. Energy-dispersive X-ray spectroscopy documented the presence of silver. The antimicrobial effect of the synthesized AgNPs revealed a significant effect against the bacteria *Klebsiella pneumonia*, *Escherichia coli*, and *Pseudomonas aeruginosa*. Additionally, cytotoxic assays showed no toxicity of AgNPs toward 3T3 mouse embryo fibroblast cells (25 µg/mL); hence, these particles were safe to use.

Keywords: antibacterial activity, *Chrysanthemum indicum*, green synthesis, silver nanoparticle, cytotoxic

Introduction

The advancement in the nanoparticle (NP) system has had an impact in scientific areas. The nature and unique properties of nanomaterials have a wide range of applications in biosensors, tissue engineering, deoxyribonucleic acid (DNA) modification, drug delivery systems, cosmetics, and medical devices.^{1–5} Silver NPs (AgNPs) are well known biocidal substances that can be incorporated as antimicrobial agents in pharmacology, veterinary medicine, implants, wound dressings, and topical ointments.^{6–9} AgNPs were also found to exhibit antibacterial and antiplatelet activities.^{10,11} This biological activity is due to the extremely small size of the NPs (1–100 nm), which enhances their physical, chemical, magnetic, and optical properties.^{12–14} The synthesis of AgNPs, through physical and chemical methods, are well known;^{15–19} however, due to their environmental impact, energy consumption, and use of toxic chemicals, the synthesis of AgNPs that uses a green approach is most preferable, as this type of approach is found to be ecofriendly and nontoxic.^{20,21} This ecofriendly approach might pave the path for researchers across the globe to explore the potential of different herbs in the synthesis of NPs. AgNPs have been reported to be green synthesized from various parts of plants such as the bark of cinnamon,²² neem leaves,²³ and various plant leaves.²⁴ Metal NPs have received great attention for their use in developing materials

for medical applications.²⁵ In recent times, several groups have reportedly achieved success in the synthesis of Au, Ag, and Pd NPs obtained from the extracts of plant parts (such as leaves);²⁶ biologically active molecules were used for the green synthesis of AgNPs of desired size and morphology using medicinal plants, bacteria, and fungi.^{27,28} These active molecules act as reducing and capping agents for the synthesis of NPs, which makes these NPs suitable for biomedical applications. Flowers are an area of interest in the synthesis of AgNPs due to their attractive carotenoid pigments. The essential oils from *Chrysanthemum indicum* flowers showed significant antimicrobial activity;²⁹ it is a well-known herbal tea in the east Asian countries and China. The whole plant is beneficial to humans, but the famous part of the plant is the flower used in chrysanthemum tea.³⁰ *C. indicum* is used in the traditional treatment of several infectious diseases such as pneumonia, colitis, stomatitis, cancer, fever, sores, and it is also used to treat vertigo, pertussis, and hypertensive symptoms.³¹ The active molecules in *C. indicum* are glycosides and flavonoids; the plant has the ability to act as antibiotic to many species of bacterial pathogens.³⁰ *C. indicum* is an herb with single, small-head, yellow daisies, which belongs to the family of *Sapotaceae*. The flowers have been consumed as tea in Chinese medicine to prevent sore throats and fevers. In traditional medicine, the flowers have been used for the treatment of dizziness, ocular inflammation, and skin boils. The flowers possess antimicrobial, anti-inflammatory, and free radical scavenging activity.^{32,33} Therefore, this work is focused on *C. indicum*. Only a few works have been carried out using the flowers *Lonicera japonica*, *Nelumbo nucifera*, and *Carthamus tinctorius*.^{34–36}

In this study, the novel, one-step biosynthesis of AgNPs using the flower extract of *C. indicum* L. at room temperature has been reported. The objective of this study is to synthesize AgNPs using a green synthesis method, and to characterize the NPs using ultraviolet–visible spectroscopy (UV–Vis), X-ray diffraction (XRD), transmission electron microscopy (TEM), and energy-dispersive X-ray spectroscopy (EDX), and to evaluate the NPs' antimicrobial effects against bacteria, as well as their in vitro cytotoxic effects on mouse embryonic fibroblast cells (3T3).

Materials and methods

Media and chemicals

Analytical-grade silver nitrate (AgNO_3) was obtained from Sigma-Aldrich (St Louis, MO, USA). All of the media components and analytical reagents were purchased from Hi-Media Laboratories Pvt Ltd (Mumbai, India).

Microorganisms and cell line

Bacillus subtilis (Microbial Type Culture Collection and Gene Bank [MTCC] 121), *Staphylococcus aureus* (MTCC 96), *S. epidermidis* (MTCC 435), *Escherichia coli* (MTCC 433), *Klebsiella pneumoniae* (MTCC 109), and *Pseudomonas aeruginosa* (MTCC 1934) were used for this experiment, and they were obtained from the Microbial Type Culture Collection (MTCC), Chandigarh, India, and the mouse embryonic fibroblast cell line (3T3) was obtained from the National Center for Cell Science (Pune, India).

Preparation of flower extract and the synthesis of AgNPs

Fresh, healthy, and disease-free *C. indicum* flowers were selected and washed repeatedly with Milli-Q deionized water (EMD Millipore, Billerica, MA, USA) to remove surface contaminants. A total of 20 g of flowers were sliced into fine pieces, and 500 mL of Milli-Q deionized water was added and then boiled for 5 minutes before decantation. The crude extract was thus obtained, and it was filtered using Whatman No 1 filter paper (Whatman plc, Kent, UK). Then, 5 mL of flower extract was assorted with 500 mL of a silver nitrate solution (1 mmol). The reaction mixture was kept undisturbed until the colorless solution converted into a reddish-brown color, which indicated the formation of AgNPs. This process was carried out at room temperature. The particles were then purified by centrifugation. To remove excess silver ions, the silver colloids were washed at least three times with deionized water. It was then lyophilized and stored in screw-capped vials under ambient conditions for further characterization and application.

Phytochemical analysis

The aqueous extract obtained from the flower of *C. indicum* was tested for the presence of the phytochemicals – tannins, saponins, flavonoids, terpenoids, steroids, alkaloids, and glycosides – according to the method described by Trease and Evans.³⁷

Characterization of NPs

UV–Vis spectroscopy

The reduction of silver ions was monitored by measuring the UV–Vis spectrum of the reaction mixture after 2 minutes by using a UV–Vis spectrophotometer (UV100; Cyberlab® Inc, Miami, FL, USA) in the wavelength ranging from 300–650 nm.

X-ray diffraction

The crystalline structures of the synthesized AgNPs were investigated by XRD. Lyophilized and powdered samples

were used, and the diffraction patterns were recorded in the scanning mode on an X'pert Pro diffractometer (PANalytical, Almelo, the Netherlands) operated at 40 kV and with a current of 30 mA, with Cu/ $k\alpha$ radiation ($\lambda=1.5418 \text{ \AA}$) in the range of 20° – 80° in 2θ angles. The average particle size of the synthesized silver AgNPs was calculated, using the Debye–Scherrer equation:

$$D = k\lambda/\beta_{1/2} \cos \theta. \quad [1]$$

Transmission electron microscope and energy dispersive X-ray analysis

TEM and EDX were performed with a JEM 1101 transmission electron microscope (JEOL, Tokyo, Japan) to confirm the size, shape, and elemental composition of the AgNPs. The sample was dispersed in ethanol on a carbon-coated copper TEM grid, and the images were obtained by operating at an accelerating voltage of 120 kV.

Antibacterial activity of synthesized AgNPs

The antibacterial efficacy was assayed by the standard Kirby–Bauer disc diffusion method³⁹ against Gram-positive and Gram-negative pathogenic bacteria. The bacterial suspension (10^8 colony-forming units/mL) was swabbed on the Mueller Hinton Agar plates using sterile cotton swabs. The sterile disc (Hi-Media Laboratories Pvt Ltd), which was 6 mm in diameter, was impregnated with the following four different components, including an aqueous extract of *C. indicum*, AgNO_3 , and synthesized AgNPs at the concentrations of 25 $\mu\text{g}/\text{disc}$. Streptomycin was used as a control. The discs were gently pressed and incubated at 37°C for 24 hours. The zone of inhibition in the diameter of each disc was measured in millimeters using a Hi-Media Laboratories Pvt Ltd. zone scale. The minimum inhibitory concentration (MIC) was determined according to the standard broth microdilution method.⁴⁰ The experiments were performed in triplicate.

Toxicity study of AgNPs

MTT assay on 3T3 cell lines

The mouse embryonic fibroblast cell line (3T3) was obtained from the National Center for Cell Science (Pune, India). The cells were seeded in a 75 cm^2 flask containing Dulbecco's Modified Eagle's Medium (DMEM) with 10% fetal bovine serum, 1.5 g/L of sodium bicarbonate, 100 U/mL of penicillin, 100 $\mu\text{g}/\text{mL}$ of streptomycin, and 0.25 $\mu\text{g}/\text{mL}$ of amphotericin B. The cell line was grown in six-well plates at a density of 5×10^4 cells/mL in DMEM,

and it was incubated to 75% confluency after 24 hours in 5% CO_2 at 37°C . The cells were then treated with synthesized AgNPs at the concentrations of 25 $\mu\text{g}/\text{mL}$ and 50 $\mu\text{g}/\text{mL}$ of growth medium. The cells were then washed with phosphate buffered saline solution thrice and stained with 3-(4,5-Dimethylthiazol-2-yl)-2,5-diphenyltetrazolium bromide (MTT) dye.⁴¹ The MTT solution (100 μL) was added to each well, followed by incubation at 37°C and 5% CO_2 for an additional 4 hours. The insoluble formazan product formed within the living cells was solubilized by adding dimethyl sulfoxide:glycine buffer (125 μL). The intensity of the solutions was measured by a microplate reader (Bio-Rad 680; Bio-Rad Laboratories, Hercules, CA, USA) with relative cell viabilities being determined as a proportion of the control. After this treatment, the cells were added to the plate and incubated for 4 hours in 5% CO_2 , at 37°C . The viability of the cells was evaluated using a microplate reader (Bio-Rad 680) at 545 nm absorbance. The absorbance is directly proportional to the number of living cells in the culture. The relative cell viability (%) related to the control wells that contained the cell culture medium without NPs as a vehicle was calculated by

$$(A) \text{ control} - (A) \text{ test}/(A) \text{ control} \times 100, \quad [2]$$

where (A) test is the absorbance of the test sample and (A) control is the absorbance of the control sample. Nontreated cells were used as the control, and the samples were imaged using an inverted photomicroscope (Nikon TE2000-E; Nikon Instruments, Melville, NY, USA).

Lactate dehydrogenase (LDH) leakage assay

The cytoplasmic enzyme release (lactate dehydrogenase [LDH]) and cell membrane instability were performed by the method of Borna et al,⁴² with minor modifications. Various concentrations (25 $\mu\text{g}/\text{mL}$ and 50 $\mu\text{g}/\text{mL}$) of the synthesized AgNPs were added to a 1 mL cuvette containing 0.9 mL of a reaction mixture to yield a final concentration of 1 mmol of pyruvate, 0.15 mmol of nicotinamide adenine dinucleotide (NADH) and 10 mmol of disodium hydrogen phosphate. After mixing thoroughly, the absorbance of the solution was measured at 340 nm. LDH activity was expressed as moles of NADH used in a minute per well.

Statistical analysis

All experiments were done in triplicate, and then the values were expressed as the mean \pm standard deviation. Statistical significance was evaluated by one-way analysis of variance followed by Student's *t*-test ($P < 0.05$), using the Statistical

Package for the Social Sciences (SPSS version 11; IBM Corporation, Armonk, NY, USA).

Results and discussion

In the present study, AgNPs were synthesized from the aqueous floral extract of *C. indicum* which acts as a reducing agent. It was observed that the reduction of silver ions into AgNPs was confirmed by the change of the silver nitrate solution to a reddish-brown color within 2 minutes at room temperature (Figure 1), whereas the control AgNO₃ solution (without the leaf extract) showed no change in color. This characteristic difference in color is due to the excitation of the surface plasmon resonance in the metal NPs.⁴³

Phytochemical analysis

The phytochemical analysis of *C. indicum* revealed the presence of tannins, flavonoids, and glycosides (Table 1). These constituents may be responsible for the formation of AgNPs by reducing AgNO₃ and acting as a capping agent to prevent agglomeration and to provide stability to the medium.⁴⁴ Flavonoids, tannins, proteins, and reducing sugars that are present in plants have been reported to act as bioreductants and capping agents.⁴⁵

UV–Vis spectroscopic analysis

The UV–Vis spectrum is one of the imperative techniques used to find low-level concentrations of metal NPs

Table 1 Phytochemical screening of the flower extract of *Chrysanthemum indicum*

Phytochemicals	<i>C. indicum</i>
Tannins	+
Saponins	–
Flavonoids	+
Terpenoids	–
Steroids	
Alkaloids	–
Glycosides	+

Notes: + Presence; – absence.

in solution. In this study, the absorption spectra were noted at 435 nm (Figure 2), and a broadening of the peak indicated that the particles were polydispersed. A similar report was observed by Loo et al.⁴⁶

XRD

The crystalline nature of the AgNPs that were synthesized using *C. indicum* was confirmed by XRD pattern analysis (Figure 3). The XRD pattern indicates the five main characteristic peaks at 2θ values of 38°, 44°, 64°, 77° and 81° corresponding to 111, 200, 220, 311 and 222 planes for silver, suggesting that these NPs were crystalline in nature.⁴⁷ The mean particle diameter of the synthesized AgNPs was calculated from the XRD pattern using Scherrer's equation:

$$D = k\lambda/\beta_{1/2} \cos \theta. \quad [3]$$

The equation uses the reference peak width at angle θ, where λ is the X-ray wavelength (1.5418 Å), β_{1/2} is the width of the XRD peak at half-height, and k is a shape factor. From this equation, the average crystalline size of the synthesized AgNPs was found to be 52 nm.

TEM and EDX analysis

The size and morphology of the synthesized AgNPs were studied by TEM (Figure 4). The size of the particles was found to be in the range of 37.71–71.99 nm, and they had a smooth surface and polydispersed particles. Figure 5 shows the clear elemental composition profile of the synthesized AgNPs. The intense signal at 3 keV strongly suggests that Ag was the major element of these NPs, as it has optical absorption in this range due to the surface plasmon resonance.⁴⁸ The other signals (carbon and oxygen) indicate the presence of plant extract, which corresponds to the biomolecules that were capping over the AgNPs.

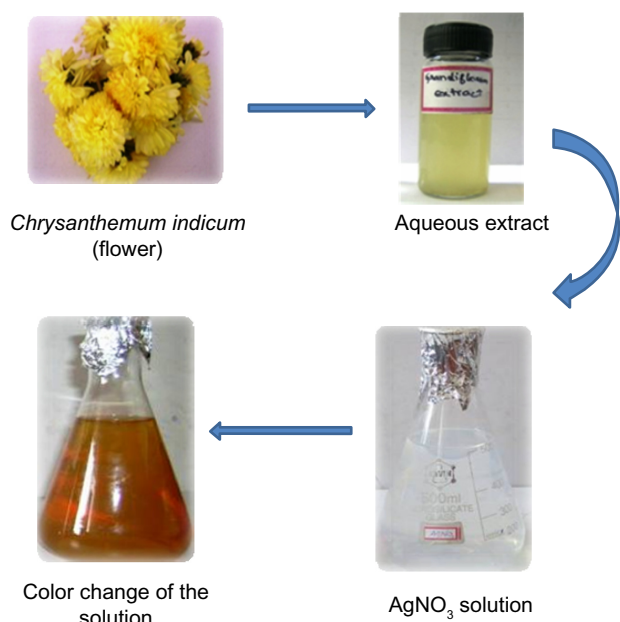


Figure 1 Schematic illustration of the green synthesis of silver nanoparticles using an aqueous extract of the *Chrysanthemum indicum* (flower).

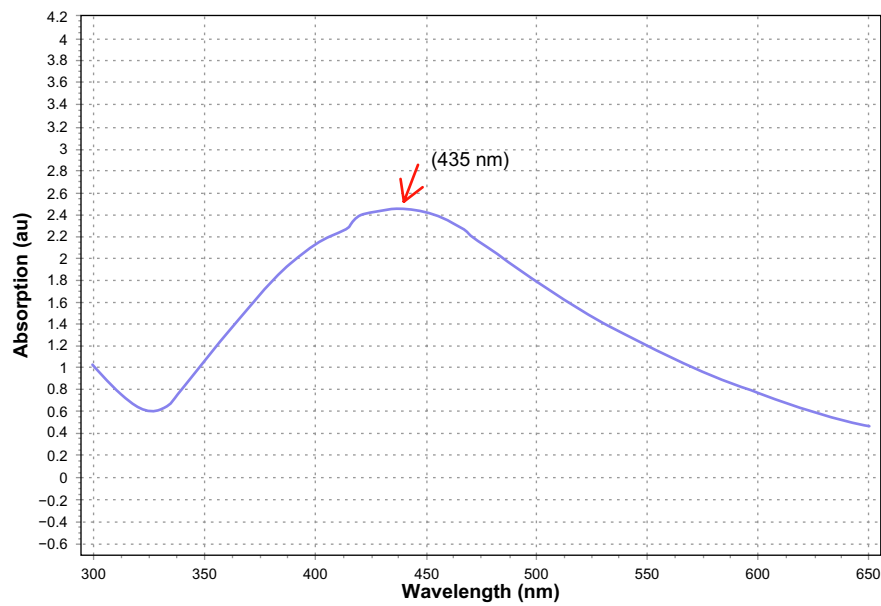


Figure 2 Ultraviolet-visible spectroscopy analysis of synthesized silver nanoparticles, and the peak noted around 435 nm.

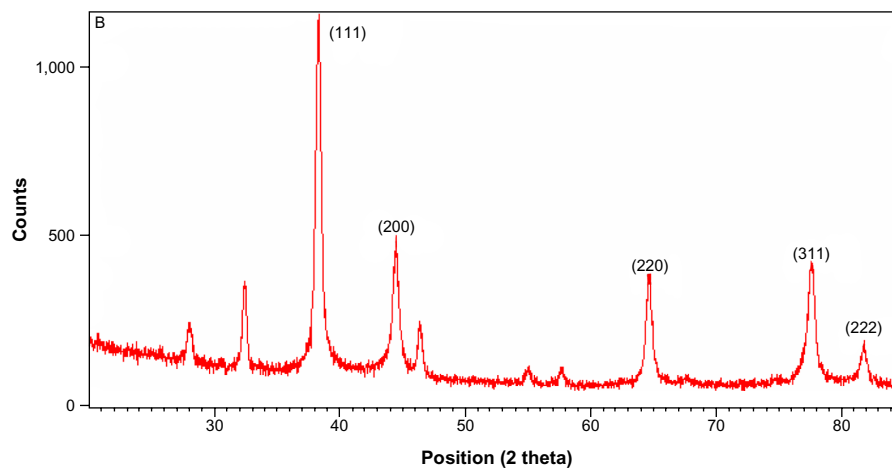


Figure 3 X-ray diffraction pattern of synthesized silver nanoparticles from the floral extract of *Chrysanthemum indicum*.

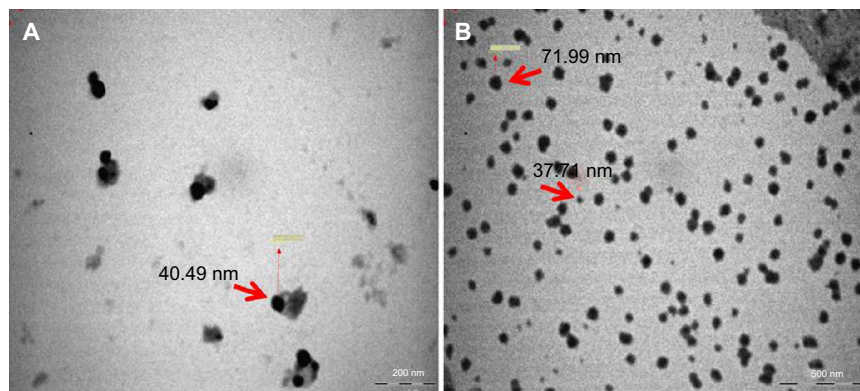


Figure 4 Transmission electron microscopy micrograph of the green synthesized silver nanoparticles.

Notes: Scale bars: (A) 200 nm and (B) 500 nm. The arrows indicate the particle size in nm.

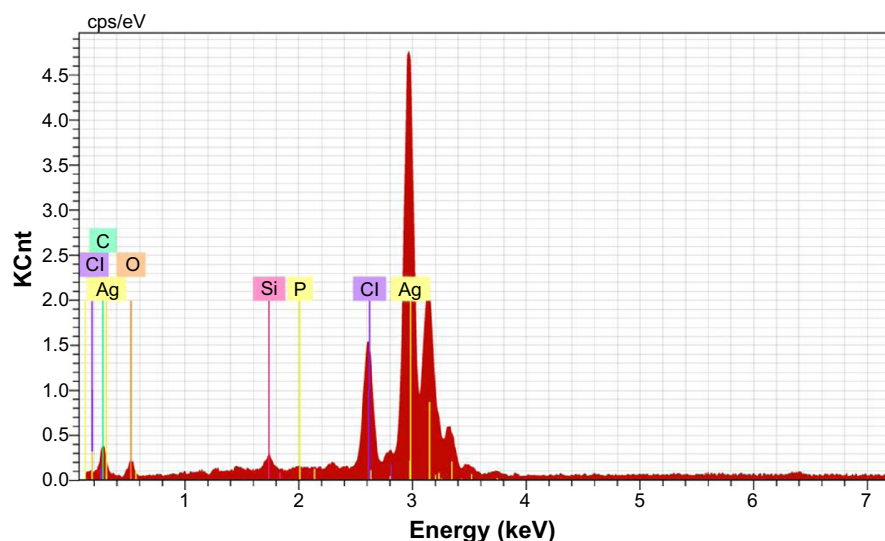


Figure 5 Energy-dispersive X-ray spectrum of green synthesized silver nanoparticles.

Antimicrobial activity of AgNPs

The antimicrobial efficacy of the aqueous floral extract of *C. indicum* and of the AgNPs was examined against three Gram-positive and three Gram-negative bacteria such as *B. subtilis* (MTCC 121), *S. aureus* (MTCC 96), *S. epidermidis* (MTCC 435), *E. coli* (MTCC 433), *K. pneumoniae* (MTCC 109), and *P. aeruginosa* (MTCC 1934). Primary screening revealed that the biologically synthesized AgNPs showed significant activity, as compared to the flower extract. The synthesized AgNPs demonstrated prominent results against *K. pneumoniae* (19 mm) *E. coli* (14 mm), and they exhibited moderate activity against *P. aeruginosa* when compared to streptomycin (Figure 6 and Table 2).

The antibacterial potential of the AgNPs in terms of their MIC are shown in Table 3. The AgNPs exhibited a MIC value of $25 \mu\text{g mL}^{-1}$ for the Gram-positive bacteria, *S. epidermidis*, and $6.25 \mu\text{g mL}^{-1}$ for the Gram-negative bacteria, *K. pneumoniae*. The MIC values of the AgNPs were slightly similar to or less than that of the standard broad spectrum antibiotic, streptomycin. This antibacterial activity exhibited by the AgNPs that were synthesized from *C. indicum* may be due to one or more of these following mechanisms. First, the effect may be due to the ultrafine size and larger surface area of the AgNPs, as their positively charged Ag^+ ions bind to the negatively charged bacterial cell wall, deactivating the cellular enzymes, causing disruptions in membrane permeability.⁴⁹ Second, interactions with the thiol group of L-cysteine protein residues may lead to enzymatic dysfunction.⁵⁰ Finally, the AgNPs may facilitate the release of reactive oxygen species, which cause damage to proteins and DNA,⁵¹ ultimately leading to cell death.

This bactericidal effect of the synthesized AgNPs may also be facilitated by the shape of AgNPs. Pal et al⁵² illustrated that the spherical and hexagonal shapes of AgNPs inhibited the Gram-negative bacterium, *E. coli*; similarly, our TEM micrographs showed spherical particles. It is noteworthy that the biologically synthesized AgNPs from *C. indicum*

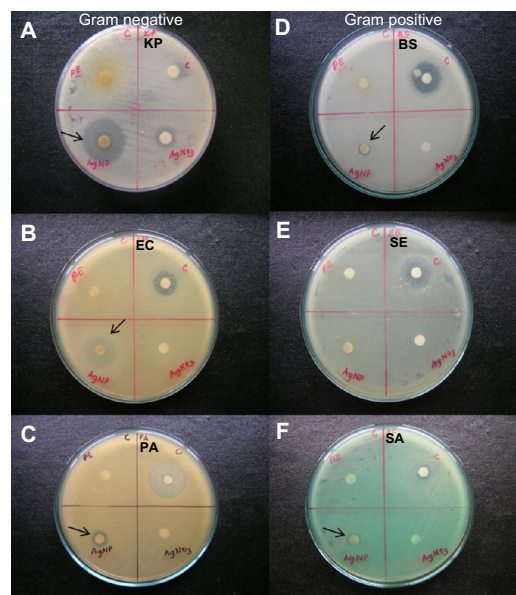


Figure 6 The antimicrobial efficacy of the aqueous extracts of *Chrysanthemum indicum*, AgNO_3 , and AgNPs were examined against three selected Gram-positive bacterial strains (D, E, and F) and three selected Gram-negative bacterial strains (A, B, and C). **Notes:** The Gram-positive bacterial strains included BS (MTCC 121), SE (MTCC 435), and SA (MTCC 96), and the three Gram-negative bacterial strains included KP (MTCC 109), EC (MTCC 433), and PA (MTCC 1934). The arrows indicate the zone of inhibition.

Abbreviations: PE, plant extract; C, control (streptomycin); KP, *Klebsiella pneumoniae*; AgNP, silver nanoparticle; EC, *Escherichia coli*; PA, *Pseudomonas aeruginosa*; BS, *Bacillus subtilis*; SE, *Staphylococcus epidermidis*; SA, *Staphylococcus aureus*; MTCC, Microbial Type Culture Collection and Gene Bank.

Table 2 Antibacterial activity of AgNPs synthesized by the aqueous flower extract of *Chrysanthemum indicum*

Indicator bacteria	Inhibitory activity (mm) ^a			
	<i>C. indicum</i> (25 µg/disc)	Silver nitrate (25 µg/disc)	AgNPs (25 µg/disc)	Streptomycin (25 µg/disc)
Gram-positive				
<i>Bacillus subtilis</i> (MTCC 121)	–	–	–	13.16±0.28
<i>Staphylococcus aureus</i> (MTCC 96)	–	–	8.33±0.57	08.12±0.57
<i>Staphylococcus epidermidis</i> (MTCC 435)	–	–	–	10.12±0.76
Gram-negative				
<i>Escherichia coli</i> (MTCC 433)	–	–	13.00±0.90	10.00±0.90
<i>Klebsiella pneumoniae</i> (MTCC 109)	–	07.00±0.50	19.10±0.50	08.00±0.50
<i>Pseudomonas aeruginosa</i> (MTCC 1934)	–	–	09.60±0.51	14.12±0.76

Notes: ^aEach value is the mean of three replicates of the diameter (mm) of the inhibition zone in the bacterial layer. Values are the means of three independent experiments. The zone of inhibition was measured after incubating the strains for 17 hours at 37°C in Muller Hinton Agar medium.

Abbreviations: AgNPs, silver nanoparticles; MTCC, Microbial Type Culture Collection and Gene Bank.

showed significant activity against Gram-negative bacteria when compared to Gram-positive bacteria. This difference was possibly due to the difference in the peptidoglycan layer. Gram-negative bacteria have a thin layer, whereas Gram-positive bacteria have a thick peptidoglycan layer (30–100 nm). As a result, the Gram-positive bacteria are defended from the bactericidal mechanisms, which are released by AgNPs.^{53,54}

Cytotoxicity of silver nanoparticles

Recently, researchers have focused on the development of methods to reduce the toxicity of AgNPs. AgNPs are toxic to both microorganisms and human cells, but when exposed to adequate concentrations, different reactions may be observed.⁵⁵ In this study, the toxicity of AgNPs synthesized from *C. indicum* were evaluated in vitro against a 3T3 mouse embryo fibroblast cell line

Table 3 Minimum inhibitory concentration of AgNPs synthesized by aqueous flower extract of *Chrysanthemum indicum*

Indicator bacteria	Minimum inhibitory concentration (µg/mL)	
	AgNPs	Streptomycin
Gram-positive		
<i>Bacillus subtilis</i> (MTCC 121)	>25	25
<i>Staphylococcus aureus</i> (MTCC 96)	>25	12.5
<i>Staphylococcus epidermidis</i> (MTCC 435)	25	>25
Gram-negative		
<i>Escherichia coli</i> (MTCC 433)	12.5	12.5
<i>Klebsiella pneumoniae</i> (MTCC 109)	6.25	25
<i>Pseudomonas aeruginosa</i> (MTCC 1934)	37.5	25

Note: Streptomycin was the control antibiotic used for the bacteria.

Abbreviations: AgNPs, silver nanoparticles; MTCC, Microbial Type Culture Collection and Gene Bank.

at 25 µg/mL and 50 µg/mL concentrations by MTT and LDH assays. In our study, the cells treated with 25 µg/mL of AgNPs did not seem to affect cell viability, which was observed to be 93.33% (Table 4). However, when the cells were treated with increased concentrations of AgNPs (50 µg/mL), they showed decreased cell viability (45.14%). The effect of AgNPs on LDH leakage in 3T3 cells are presented in Table 4. From the results, it is clear that there was no significant increase in LDH at 25 µg/mL (0.12 µmol/NADH) when compared to control, but there is an increase in LDH activity of 0.42 µmol/NADH at a concentration of 50 µg/mL. The toxicity of the synthesized AgNPs depends on their dose. Investigations of the morphological features of treated cells using an inverted microscope revealed that changes in the cell morphology were clearly reflected at 50 µg/mL when compared to the cells treated at concentrations of 25 µg/mL (Figure 7). It can be clearly observed that the cells treated with AgNPs (25 µg/mL) have a well-developed nucleus, devoid of peripheral cellular distribution. Conversely, in the cells treated with a concentration of 50 µg/mL, systematic changes in the morphological features of the cells occurred. Further, with the LDH assay, a rise in

Table 4 Cell viability and LDH leakage in control- and AgNP-treated 3T3 cells after 24 hours of exposure

Concentration (µg/mL)	Percentage of viability	LDH activity (µmol/NADH/well/minute)
25	93.33±1.45*	0.12±0.007*
50	45.14±1.38*	0.42±0.003*
Control	97.70±1.49	0.11±0.005

Notes: The values represent the mean ± standard deviation of two independent experiments. *P<0.001 versus control.

Abbreviations: LDH, lactate dehydrogenase; AgNP, silver nanoparticle; NADH, nicotinamide adenine dinucleotide.

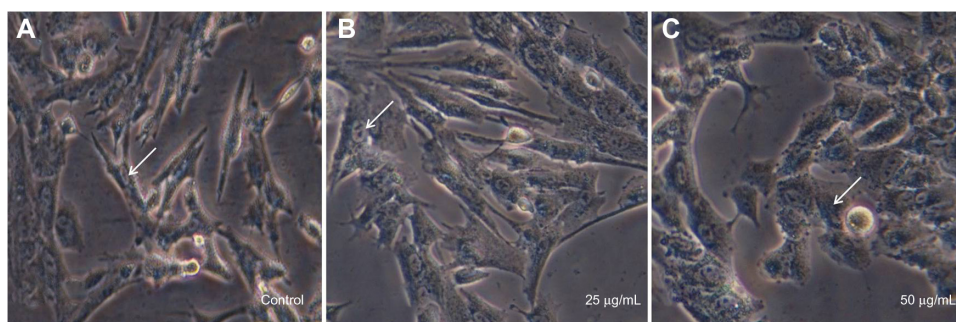


Figure 7 Cytotoxicity of synthesized silver nanoparticles on 3T3 mouse embryo fibroblast cells.

Notes: (A) Control (cell + phosphate buffered saline); (B) cell +25 µg/mL of silver nanoparticles; (C) cell +50 µg/mL of silver nanoparticles. The arrows indicate the cell nucleus.

LDH enzyme activity was observed at 50 µg/mL when compared to the control cells. LDH is a stable cytoplasmic enzyme that is present in most of the eukaryotic cells, and it is secreted into the culture medium during the damage or rupture of the cell's cytoplasmic membrane. The elevated levels of LDH enzyme activity are directly proportional to the number of dead or damaged plasma membrane cells.⁵⁶ In this study, the synthesized AgNPs from the aqueous flower extract of *C. indicum* were found to exhibit highly antibacterial activity against *K. pneumoniae* and *E. coli* at concentrations of 25 µg/mL, and no cytotoxic effects on mouse embryonic fibroblast cells were observed. This result may provide a safe start for the use of AgNPs in pharmaceutical and other medical applications.

Conclusion

The present study reported on the synthesis of AgNPs by *C. indicum* without using any harmful reducing or capping agents, as confirmed by UV-Vis spectrophotometer, XRD, TEM, and EDX techniques. Spherical, smooth surface, and poly-dispersed particles of sizes ranging from 37.71–71.99 nm with an average size of 52.9±4.6 nm were obtained. The lowest MIC of the AgNPs was exhibited against *E. coli* and *K. pneumoniae* (12.5 µg/mL and 6.25 µg/mL, respectively). The synthesized AgNPs act as excellent bactericidal agents, without exhibiting any toxic effects on mouse embryonic fibroblast cells.

Acknowledgments

The authors gratefully acknowledge the National Institute of Animal Science, Republic of Korea, for supporting this research. In addition, thanks to CERD, Loyola College, Chennai, India for providing the laboratory facilities.

Disclosure

The authors report no conflicts of interest in this work.

References

- Kotthaus S, Gunther BH, Hang R, Schafer H. Study of isotropically conductive bondings filled with aggregates of nano-sited Ag-particles. *IEEE Trans Compon Packaging Manuf Technol*. 1997;20(1):15–20.
- Klaus-Joerger T, Joerger R, Olsson E, Granqvist C. Bacteria as workers in the living factory: metal-accumulating bacteria and their potential for materials science. *Trends Biotechnol*. 2001;19(1):15–20.
- Goldsmith BR, Mitala JJ, Josue J, et al. Biomimetic chemical sensors using nanoelectronic readout of olfactory receptor proteins. *ACS Nano*. 2011;5(7):5408–5416.
- Tolaymat TM, El Badawy AM, Genaidy A, Scheckel KG, Luxton TP, Suidan M. An evidence-based environmental perspective of manufactured silver nanoparticle in syntheses and applications: a systematic review and critical appraisal of peer-reviewed scientific papers. *Sci Total Environ*. 2010;408(5):999–1006.
- Weir A, Westerhoff P, Fabricius L, Hristovski K, von Goetz N. Titanium dioxide nanoparticles in food and personal care products. *Environ Sci Technol*. 2012;46(4):2242–2250.
- Kim KJ, Sung WS, Suh BK, et al. Antifungal activity and mode of action of silver nano-particles on *Candida albicans*. *Biometals*. 2009;22(2):235–242.
- Nadworny PL, Wang J, Tredget EE, Burrell RE. Anti-inflammatory activity of nanocrystalline silver-derived solutions in porcine contact dermatitis. *J Inflamm (Lond)*. 2010;7:13.
- Lara HH, Ayala-Núñez NV, Ixtapan-Turrent L, Rodríguez-Padilla C. Mode of antiviral action of silver nanoparticles against HIV-1. *J Nanobiotechnology*. 2010;8:1.
- Becker RO. Silver ions in the treatment of local infections. *Met Based Drugs*. 1999;6(4–5):311–314.
- Xiu ZM, Zhang QB, Puppala HL, Colvin VL, Alvarez PJ. Negligible particle-specific antibacterial activity of silver nanoparticles. *Nano Lett*. 2012;12(8):4271–4275.
- Shrivastava S, Bera T, Singh SK, Singh G, Ramachandrarao P, Dash D. Characterization of antiplatelet properties of silver nanoparticles. *ACS Nano*. 2009;3(6):1357–1364.
- Bogunia-Kubik K, Sugisaka M. From molecular biology to nanotechnology and nanomedicine. *Biosystems*. 2002;65(2–3):123–138.
- Zharov VP, Kim JW, Curiel DT, Everts M. Self-assembling nanoclusters in living systems: application for integrated photothermal nanodiagnosics and nanotherapy. *Nanomedicine*. 2005;1(4):326–345.
- Dobrovolskaia MA, McNeil SE. Immunological properties of engineered nanomaterials. *Nat Nanotechnol*. 2007;2(8):469–478.
- Kruis FE, Fissan H, Rellinghaus B. Sintering and evaporation characteristics of gas-phase synthesis of size-selected PbS nanoparticles. *Materials Science and Engineering: B*. 2000;69–70:329–334.
- Mafuné F, Kohno JY, Takeda Y, Kondow T. Formation and size control of silver nanoparticles by laser ablation in aqueous solution. *J Phys Chem B*. 2000;104(39):9111–9117.
- Wiley B, Sun Y, Mayers B, Xia Y. Shape-controlled synthesis of metal nanostructures: the case of silver. *Chemistry*. 2005;11(2):454–463.

18. Merga G, Wilson R, Lynn G, Milosavljevic BH, Meisel D. Redox catalysis on “naked” silver nanoparticles. *J Phys Chem C Nanomater Interfaces*. 2007;111(33):12220–12226.
19. Oliveira MM, Ugarte D, Zanchet D, Zarbin AJ. Influence of synthetic parameters on the size, structure, and stability of dodecanethiol-stabilized silver nanoparticles. *J Colloid Interface Sci*. 2005;292(2):429–435.
20. Ankamwar B, Damle C, Ahmad A, Sastry M. Biosynthesis of gold and silver nanoparticles using *Emblca officinalis* fruit extract, their phase transfer and transmetallation in an organic solution. *J Nanosci Nanotechnol*. 2005;5(10):1665–1671.
21. Geethalakshmi R, Sarada DV. Gold and silver nanoparticles from *Trianthema decandra*: synthesis, characterization, and antimicrobial properties. *Int J Nanomedicine*. 2012;7:5375–5384.
22. Sathishkumar M, Sneha K, Won SW, Cho CW, Kim S, Yun YS. Cinnamon zeylanicum bark extract and powder mediated green synthesis of nano-crystalline silver particles and its bactericidal activity. *Colloids Surf B Biointerfaces*. 2009;73(2):332–338.
23. Tripathi A, Chandrasekaran N, Raichur AM, Mukherjee A. Antibacterial applications of silver nanoparticles synthesized by aqueous extract of *Azadirachta indica* (Neem) leaves. *J Biomed Nanotechnol*. 2009;5(1):93–98.
24. Song JY, Kim BS. Rapid biological synthesis of silver nanoparticles using plant leaf extracts. *Bioprocess Biosyst Eng*. 2009;32(1):79–84.
25. Shahverdi AR, Fakhimi A, Shahverdi HR, Minaian S. Synthesis and effect of silver nanoparticles on the antibacterial activity of different antibiotics against *Staphylococcus aureus* and *Escherichia coli*. *Nanomedicine*. 2007;3(2):168–171.
26. Shankar SS, Ahmad A, Sastry M. Geranium leaf assisted biosynthesis of silver nanoparticles. *Biotechnol Prog*. 2003;19(6):1627–1631.
27. Ghosh S, Patil S, Ahire M, et al. Synthesis of silver nanoparticles using *Dioscorea bulbifera* tuber extract and evaluation of its synergistic potential in combination with antimicrobial agents. *Int J Nanomedicine*. 2012;7:483–496.
28. Prakash P, Gnanaprakasam P, Emmanuel R, Arokiyaraj S, Saravanan M. Green synthesis of silver nanoparticles from leaf extract of *Mimusops elengi*, Linn. for enhanced antibacterial activity against multi drug resistant clinical isolates. *Colloids Surf B Biointerfaces*. 2013;108:255–259.
29. Shunying Z, Yang Y, Huaidong Y, Yue Y, Guolin Z. Chemical composition and antimicrobial activity of the essential oils of *Chrysanthemum indicum*. *J Ethnopharmacol*. 2005;96(1–2):151–158.
30. Jung EK. Chemical composition and antimicrobial activity of the essential oil of *Chrysanthemum indicum* against oral bacteria. *Journal of Bacteriology and Virology*. 2009;39(2):61–69.
31. Pitinidhipat N, Yasurin P. Antibacterial activity of *Chrysanthemum indicum*, *Cantella asiatica* and *Andrographis paniculata* against *Bacillus cereus* and *Listeria monocytogenes* under osmotic stress. *Assumption University Journal of Technology*. 2012;15(4):239–245.
32. Cheng W, Li J, You T, Hu C. Anti-inflammatory and immunomodulatory activities of the extracts from the inflorescence of *Chrysanthemum indicum* Linné. *J Ethnopharmacol*. 2005;101(1–3):334–337.
33. Pongjit C, Ninsontia C, Chaotham, Chanvorachote P. Protective effect of Glycine max and *Chrysanthemum indicum* extracts against cisplatin-induced renal epithelial cell death. *Human Exp Toxicol*. 2011;30(12):1931–1944.
34. Nagajyothi PC, Lee SE, An M, Lee KD. Green synthesis of silver and gold nanoparticles using *Lonicera japonica* flower extract. *Bull Korean Chem Soc*. 2012;33(8):2609–2612.
35. Arokiyaraj S, Udaya Prakash NK, Vijay Elakky, Kamala T, Bhuvanewari S, Dinesh Kumar V. Green synthesis of silver nanoparticles using aqueous floral extract of *Nelumbo Nucifera*. *Materials Science Forum*. 2013;756:106–111.
36. Sreekanth TVM, Lee KD. Green synthesis of silver nanoparticles from *Carthamus tinctorius* flower extract and evaluation of their antimicrobial and cytotoxic activities. *Curr Nanosci*. 2011;7(6):1046–1053.
37. Trease GE, Evans WC. *Pharmacognosy*. 11th ed. London: Bailliere Tindall; 1989: 45–50.
38. Amin M, Anwar F, Janjua MR, Iqbal MA, Rashid U. Green synthesis of silver nanoparticles through reduction with *Solanum xanthocarpum* L. berry extract: characterization, antimicrobial and urease inhibitory activities against *Helicobacter pylori*. *Int J Mol Sci*. 2012;13(8):9923–9941.
39. Bauer AW, Kirby WM, Sherris JC, Turck M. Antibiotic susceptibility testing by a standardized single disk method. *Am J Clin Pathol*. 1966;45(4):493–496.
40. Clinical and Laboratory Standards Institute. *Methods for Determining Bactericidal Activity of Antimicrobial Agents; Approved Guideline*. Wayne, PA: Clinical and Laboratory Standards Institute; 1999.
41. Mosmann T. Rapid colorimetric assay for cellular growth and survival: application to proliferation and cytotoxicity assays. *J Immunol Methods*. 1983;65(1–2):55–63.
42. Borna S, Abdollahi A, Mirzaei F. Predictive value of mid-trimester amniotic fluid high-sensitive C-reactive protein, ferritin, and lactate dehydrogenase for fetal growth restriction. *Indian J Pathol Microbiol*. 2009;52(4):498–500.
43. Krishnaraj C, Jagan EG, Rajasekar S, Selvakumar P, Kalaichelvan PT, Mohan N. Synthesis of silver nanoparticles using *Acalypha indica* leaf extracts and its antibacterial activity against water borne pathogens. *Colloids Surf B Biointerfaces*. 2010;76(1):50–56.
44. Jha AK, Prasad K, Prasad K, Kulkarni AR. Plant system: nature’s nanofactory. *Colloids Surf B Biointerfaces*. 2009;73(2):219–223.
45. Li S, Shen Y, Xie A, et al. Green synthesis of silver nanoparticles using *Capsicum annuum* L. extract. *Green Chemistry*. 2007;9:852–858.
46. Loo YY, Chieng BW, Nishibuchi M, Radu S. Synthesis of silver nanoparticles by using tea leaf extract from *Camellia sinensis*. *Int J Nanomedicine*. 2012;7:4263–4267.
47. Khan M, Khan M, Adil SF, et al. Green synthesis of silver nanoparticles mediated by *Pulicaria glutinosa* extract. *Int J Nanomedicine*. 2013;8:1507–1516.
48. Najitha Banu A, Balasubramanian C, Moorthi PV. Biosynthesis of silver nanoparticles using *Bacillus thuringiensis* against dengue vector, *Aedes aegypti* (Diptera: Culicidae). *Parasitol Res*. Epub 2013 Oct 31.
49. Su HL, Chou CC, Hung DJ, et al. The disruption of bacterial membrane integrity through ROS generation induced by nanohybrids of silver and clay. *Biomaterials*. 2009;30(30):5979–5987.
50. Gordon O, Vig Slenters T, Brunetto PS, et al. Silver coordination polymers for prevention of implant infection: thiol interaction, impact on respiratory chain enzymes, and hydroxyl radical induction. *Antimicrob Agents Chemother*. 2010;54(10):4208–4218.
51. Hossain Z, Huq F. Studies on the interaction between Ag(+) and DNA. *J Inorg Biochem*. 2002;91(2):398–404.
52. Pal S, Tak YK, Song JM. Does the antibacterial activity of silver nanoparticles depend on the shape of the nanoparticle? A study of the Gram-negative bacterium *Escherichia coli*. *Appl Environ Microbiol*. 2007;73(6):1712–1720.
53. Saravanan M, Vemu AK, Barik SK. Rapid biosynthesis of silver nanoparticles from *Bacillus megaterium* (NCIM 2326) and their antibacterial activity on multi drug resistant clinical pathogens. *Colloids Surf B Biointerfaces*. 2011;88(1):325–331.
54. Kim SH, Lee HS, Ryu DS, Choi SJ, Lee DS. Antibacterial activity of silver-nanoparticles against *Staphylococcus aureus* and *Escherichia coli*. *Korean Journal of Microbiology and Biotechnology*. 2011;39(1):77–85.
55. You C, Han C, Wang X, et al. The progress of silver nanoparticles in the antibacterial mechanism, clinical application and cytotoxicity. *Mol Biol Rep*. 2012;39(9):9193–9201.
56. Sasaki T, Kawai K, Saijo-Kurita K, Ohno T. Detergent cytotoxicity: simplified assay of cytolysis by measuring LDH activity. *Toxicol In Vitro*. 1992;6(5):451–457.

International Journal of Nanomedicine

Dovepress

Publish your work in this journal

The International Journal of Nanomedicine is an international, peer-reviewed journal focusing on the application of nanotechnology in diagnostics, therapeutics, and drug delivery systems throughout the biomedical field. This journal is indexed on PubMed Central, MedLine, CAS, SciSearch®, Current Contents®/Clinical Medicine,

Journal Citation Reports/Science Edition, EMBase, Scopus and the Elsevier Bibliographic databases. The manuscript management system is completely online and includes a very quick and fair peer-review system, which is all easy to use. Visit <http://www.dovepress.com/testimonials.php> to read real quotes from published authors.

Submit your manuscript here: <http://www.dovepress.com/international-journal-of-nanomedicine-journal>